Available online at www.sciencedirect.com
SCIENCE DIRECT®
ELSEVIER
Microelectronic Engineering 75 (2004) 269–274
MICROELECTRONIC ENGINEERING
www.elsevier.com/locate/mee

Experimental and theoretical investigation of MEH-ppv based Schottky diodes

Mo Zhu [a], Tianhong Cui [b], Kody Varahramyan [a,*]

[a] *Institute for Micromanufacturing, Louisiana Tech University, 911 Hergot Avenue, Ruston, LA 71272, USA*
[b] *Mechanical Engineering and Nanofabrication Center, University of Minnesota, Minneapolis, MN 55455, USA*

Received 4 February 2004; received in revised form 4 May 2004; accepted 26 May 2004
Available online 2 July 2004

Abstract

MEH-PPV (poly[2-methoxy-5-(2′-ethyl-hexyloxy)-1,4-phenylene vinylene]) based Schottky diodes have been fabricated and investigated through the analyses of current density–voltage and capacitance–voltage characteristics. Temperature-dependent hole mobility of MEH-PPV is extracted by the space-charge limited conduction (SCLC) model from 300 to 400 K, and the use of the SCLC model is examined in high electric field. The highest measured hole mobility is 0.013 cm^2/Vs at 353 K. The thickness of MEH-PPV in the structures consisting of ITO/MEH-PPV/Al, largely affects the performance of the diodes, and the thinner film displays better device performance. According to capacitance–voltage relations, the effective carrier density and Schottky barrier height of MEH-PPV have been determined to be 2.24×10^{17} cm^{-3} and 0.64 eV, respectively.

Keywords: Polymer Schottky diodes; MEH-PPV; SCLC; Mobility

1. Introduction

Recently organic materials have been widely investigated due to their attractive applications in microelectronic and optoelectronic devices, such as organic thin film transistors (OTFTs) and organic light emitting diodes (OLEDs) [1–4]. MEH-PPV (poly[2-methoxy-5-(2′-ethyl-hexyloxy)-1,4-phenylene vinylene]) is poly(para-phenylene vinylene) (PPV) derivated p-type polymer which is among the most popular materials used to build OTFTs and OLEDs [5–7]. Several studies have been carried out for Schottky diodes by MEH-PPV and various metals [8–10]. The characteristics of Schottky contact between polymer and metal are important to investigate both material properties and interface characteristics. Temperature and electric field dependent mobility of MEH-PPV was studied in [11,12]. However, the mobility

* Corresponding author. Tel.: +1-318-257-5107; fax: +1-318-257-5104.
E-mail address: kody@latech.edu (K. Varahramyan).

0167-9317/$ - see front matter
doi:10.1016/j.mee.2004.05.011

behavior of MEH-PPV above room temperature does not seem to have been reported. In this work, experimental and theoretical efforts have been carried out to investigate the mobility behavior above room temperature, based on the current density–voltage (*J–V*) characteristics and capacitance–voltage (*C–V*) characteristics of ITO/MEH-PPV/Al Schottky diodes. The space-charge limited conduction (SCLC) model [13] and the field-dependent relationship have been employed to extract mobility values.

2. Models

The SCLC model [11,13] has been widely used to describe the behavior of organic diodes. But the SCLC model is limited for low electric field conditions. With the increase in electric field, the SCLC model ignores the field-dependent mobility. Thus the field-dependent relationship is used to more accurately describe the behavior of devices at high electric fields.

2.1. SCLC model

SCLC model was proposed for the bulk transport dominated conduction processes in OLEDs [14], which describes the current limited by the space charge. In other words, the density of free carriers injected into the active region is larger than the number of acceptor levels (assumed p-type material). For organic materials, the SCLC model is expected to be applicable due to relatively small acceptor density and small mobility of the carriers. The model is described by the following equation

$$J = \frac{9}{8}\varepsilon_0\varepsilon_r\mu_p\frac{V^2}{L^3}, \tag{1}$$

where J is current density, V is voltage, $\varepsilon_0\varepsilon_r$ is permittivity of the polymer, μ_p is the hole mobility (assumed p-type conducting polymer), and L is the device thickness.

The SCLC regime occurs when the equilibrium charge concentration (before charge injection) is negligible compared to the injected charge concentration. This will form a space charge region near the injecting electrode; with the concentration of the space charge rapidly ending away from the electrode. In this regime, the current is proportional to the square of the electric field.

2.2. Field-dependent relationship

Field-dependent models are used to describe the hole mobility in MEH-PPV when the electric field is high, and the constant mobility in the SCLC model is no longer applicable. The characteristics of current density versus voltage can be described by the equation

$$J = p(x)e\mu_p[E(x)]E(x), \tag{2}$$

with the field-dependent mobility given by

$$\mu_p(E) = \mu_p(0)\exp(\gamma\sqrt{E}), \tag{3}$$

where the zero field mobility is given by

$$\mu_p(0) = \mu_0\exp\left(-\frac{E^*}{k_B T}\right) \tag{4}$$

and

$$\gamma = B\left(\frac{1}{k_B T} - \frac{1}{k_B T_0}\right), \tag{5}$$

where $p(x)$ is the density of hole concentration at position x, $E(x)$ is the electric field at position x, μ_0 is a constant prefactor, E^* is the activation energy, and T_0 and B are material constants.

3. Experimental

MEH-PPV (American Dye Source, Inc.) 0.2 wt% solution was prepared on tetrahydrofuran glass substrate covered by a deposited layer of ITO thin film. After substrate cleaning by acetone and deionized water, MEH-PPV was deposited on the ITO/glass substrate by spin-coating technique. After baking at 200 °C for 20 min, a 200 nm layer of Al was deposited on MEH-PPV through thermal evaporation at a pressure of 1×10^{-6} Torr. Subsequently, the Al and MEH-PPV were patterned by traditional lithography and reactive ion etching (RIE) technique using the same mask. Thus, Schottky diodes were formed with ITO as bottom electrode, Al as top

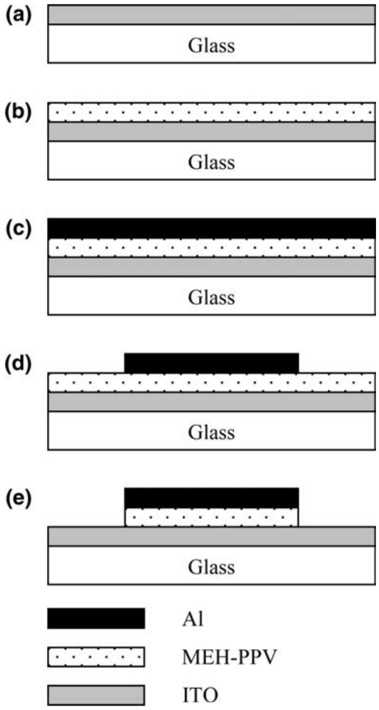

Fig. 1. Fabrication steps of the MEH-PPV based Schottky diodes.

electrode, and MEH-PPV as active material. The thickness of MEH-PPV is 200 nm (tested by Tencor Alphastep 500 Surface Profiler). Fig. 1 schematically shows the fabrication procedure used and the structure of the MEH-PPV based diodes (Fig. 1(e)).

A Keithley Test Station (236 Source Measure Unit and 590 *C–V* Analyzer) was used to test the fabricated devices from 300 to 400 K. At different temperatures, *J–V* and *C–V* characteristics were measured for the fabricated devices, and key parameters, as hole mobility and carrier density were calculated.

4. Results and discussion

4.1. Mobility

MEH-PPV and Al form Schottky contact at their interface and generate a depletion region in

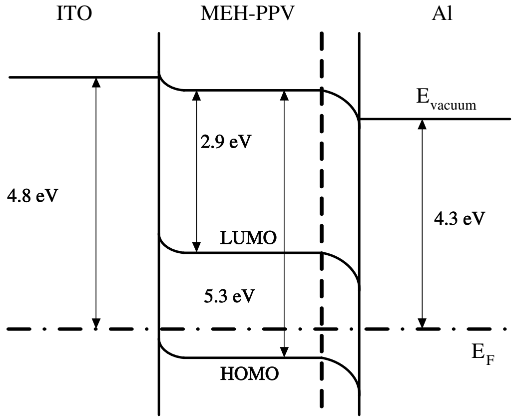

Fig. 2. Energy-band alignment of the ITO/MEH-PPV/Al structure.

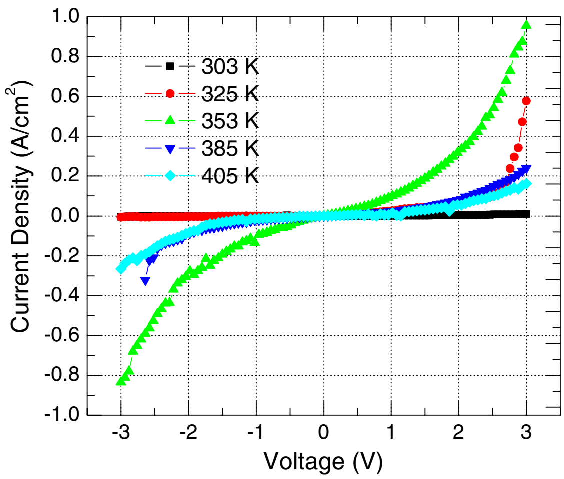

Fig. 3. Current density–voltage characteristics of ITO/MEH-PPV/Al Schottky diode at different temperatures.

MEH-PPV, as shown in Fig. 2 [15]. When the forward voltage is applied, the barrier height at the interface decreases, turning on the device. At reverse voltage, the barrier height increases to block the current. The *J–V* characteristics at different temperatures are shown in Fig. 3. The J–V^2 characteristics at forward voltage are provided in Fig. 4 for 325, 353 and 385 K, showing both the experimental (dot) and theoretical (solid line) results. The theoretical results have been calculated from the SCLC model (Eq. (1), using $L = 200$ nm

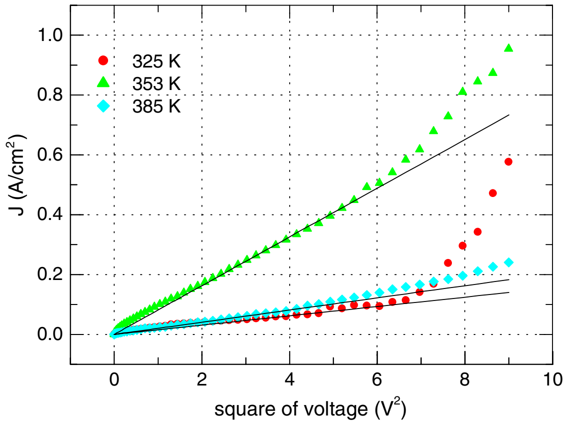

Fig. 4. J–V^2 characteristics of ITO/MEH-PPV/Al diode at $V_{ITO/Al} > 0$ V, at different temperatures. The theoretical results based on the SCLC model are also shown (solid lines).

and assuming $\varepsilon_0 = 3$ [11]. These results match well the experimental data at low electric field conditions. With the increase in electric field, the SCLC model underestimates the hole mobility in MEH-PPV, by ignoring the high field effects, which may be described by Eq. (3).

The mobility–temperature plot extracted from the SCLC model at near zero electric-field is shown in Fig. 5. The hole mobility of MEH-PPV increases from 300 to 350 K, which fits the exponential relation in Eq. (4). Above 350 K, the mobility drops to a lower value, which is attributed to the degradation of MEH-PPV as a conducting polymer, and the increase in carrier scattering with the rise in temperature. When the temperature is lowered back, almost the same J–V characteristics are measured, demonstrating that no annealing effect exists. The behavior of hole mobility in the regime it increases with temperature can be exponentially described by Eq. (4), with the values of μ_0 and E^* determined to be 4.13×10^{-9} cm^2/Vs and 0.451 eV, respectively.

4.2. Device performance

As shown in Fig. 3, the device performance starts degrading at about 350 K, though a higher mobility is reached. At higher temperatures, the leakage current becomes very large and the device acts more as a resistor instead of a diode. Fig. 6 shows the detailed plot of J–V characteristics at 325 K, as an example, where significant mobility is obtained as well as relatively lower leakage current. The best ideality factor of 10.7 is obtained at 325 K, according to the classic model which describes the behavior of Schottky diodes under forward bias [16]

$$I = I_0(e^{V/n\phi_T} - 1), \tag{6}$$

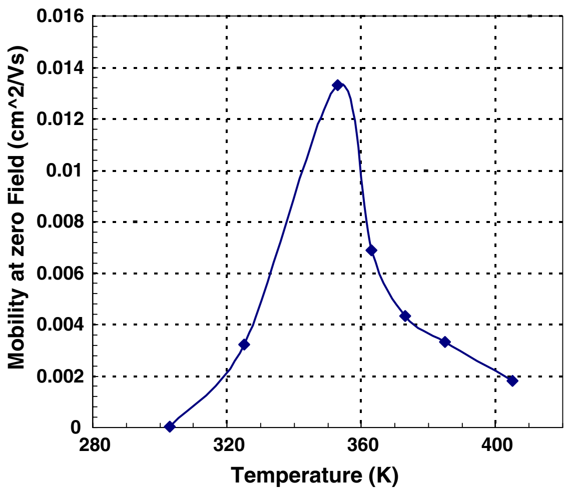

Fig. 5. Extracted hole mobility in MEH-PPV, at near zero electric field, as a function of temperature.

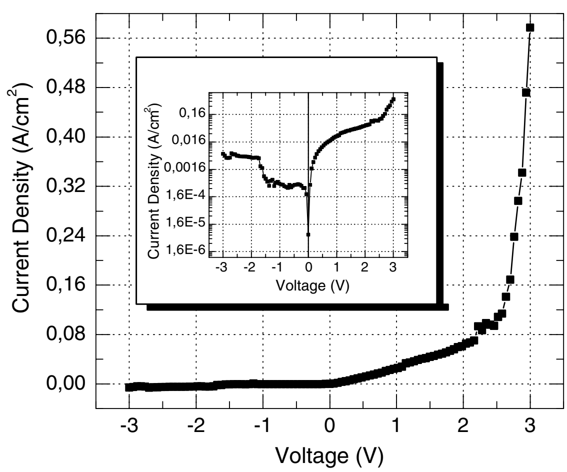

Fig. 6. Current density–voltage characteristics of ITO/MEH-PPV/Al diode at 325 K.

where n is ideality factor, I_0 is reverse leakage current, and ϕ_T is the thermal voltage at certain temperature. At other temperatures, the ideality factor is much higher (e.g. 35.5 at 353 K). This suggests that the optimal operating temperature of fabricated Schottky diodes is around 325 K with respected to leakage current and diode behavior, though the highest mobility is not obtained at this point. Compared to the ideality factor for inorganic semiconductors, for example 1.02 for silicon diodes [16], the ideality factor of MEH-PPV diodes is much larger due to the high resistivity of the organic material.

Another factor affecting the device performance is the thickness of the active layer. As shown by the J–V curves in Fig. 7, there is noticeable difference between the two devices considered, one with 70 nm and the other with 200 nm thick layer of MEH-PPV, measured at room temperature. The performance of the 70 nm MEH-PPV device appears much better than that of one with 200 nm MEH-PPV.

4.3. Charge distribution

Capacitance–voltage measurements allow extraction of the effective carrier density and barrier height in the given devices. The following relation [17,18] is normally used to extract the carrier density in solid materials:

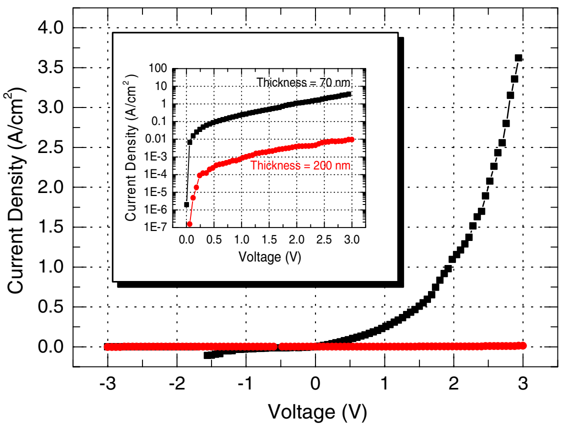

Fig. 7. Current density–voltage characteristics of ITO/MEH-PPV/Al diodes with film thickness of 200 and 70 nm, respectively.

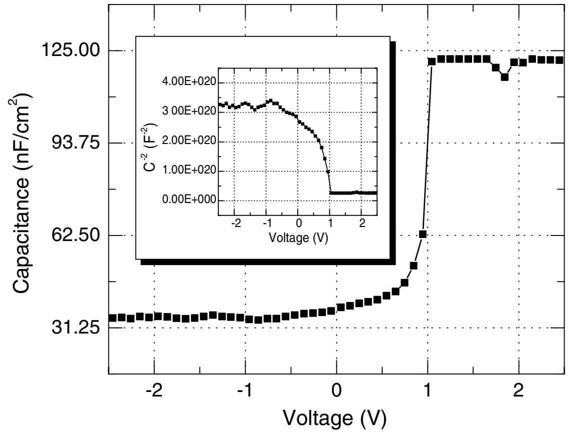

Fig. 8. Capacitance–voltage characteristics of ITO/MEH-PPV/Al diode at high frequency (100 kHz).

$$N = \frac{-2\Delta V}{q\varepsilon_0\varepsilon_r A^2 \Delta(1/C^2)}, \quad (7)$$

where N is the carrier density and A the device area.

Capacitance–voltage characteristics of the ITO/MEH-PPV/Al diode, at high frequency (100 kHz), are shown in Fig. 8, with C^{-2}–V plot inserted. At linear region near zero bias voltage, the calculated effective carrier density is 2.24×10^{17} cm^{-3} at room temperature and in good agreement with the findings in [19]. The non-linear region of the C^{-2}–V characteristics demonstrates non-uniform distribution of concentration in the MEH-PPV due to interface state and irregular surface profile [20]. Assuming that the mobility-independent trap level is 1×10^{21} cm^{-3} [15] and the difference of work function and the highest occupied molecular orbital (HOMO) level is 0.36 eV, the barrier height can be calculated to be 0.64 eV at room temperature, which is consistent with the results obtained in [12,21].

5. Conclusions

In summary, the electrical properties of MEH-PPV, including temperature-dependent mobility, have been experimentally and theoretically investigated based on current density–voltage and capacitance–voltage characteristics of ITO/MEH-PPV/Al Schottky diodes. As part of this work, the

SCLC model and the field-dependent mobility model have been examined. At 353 K, an effective carrier density of 2.24×10^{17} cm^{-3} and the highest mobility value of 0.013 cm^2/Vs have been obtained. Moreover, the barrier height has been determined to be 0.64 eV at room temperature.

Acknowledgements

The authors acknowledge the laboratory and technical resources provided by the Institute for Micromanufacturing for the realization of this work. They thank Mr. D. Tatum for technical support, and Drs. G. Liang and J. Wang for helpful discussions. This work was supported in part by a DARPA grant.

References

[1] J.M. Shaw, P.F. Seidler, IBM J. Res. Dev. 45 (2001) 3.
[2] H. Klauk, T.N. Jackson, Solid State Tech. 43 (2000) 63.
[3] A. Curioni, W. Andreoni, IBM J. Res. Dev. 45 (2001) 101.
[4] P.W.M. Blom, M.J.M. De Jong, Philips J. Res. 51 (1998) 479.
[5] J. Yoon, J. Kim, T. Lee, O. Park, Appl. Phys. Lett. 76 (2000) 2152.
[6] T.P. Nguyen, P.L. Rendu, N.N. Dihn, M. Fourmigue, C. Meziere, Synth. Met. 138 (2003) 229.
[7] Y. Roichman, N. Tessler, Appl. Phys. Lett. 80 (2002) 151.
[8] S.J. Martin, J.M. Lupton, I.D.W. Samuel, A.B. Walker, J. Phys.: Condens. Matter. 14 (2002) 9925.
[9] J.C. Scott, G.G. Malliaras, W.D. Chen, J. Breach, J.R. Salem, P.J. Brock, S.B. Sachs, C.E.D. Chidsey, Appl. Phys. Lett. 74 (1999) 1510.
[10] J. Yang, I. Shalish, Y. Shapira, Phys. Rev. B 64 (2001) 035325.
[11] P.W.M. Blom, M.J.M. de Jong, M.G. van Munster, Phys. Rev. B 55 (1997) R656.
[12] J.M. Lupton, I.D.W. Samuel, Synth. Met. 111–112 (2000) 381.
[13] A.J. Campbell, D.D.C. Bradley, D.G. Lidzey, J. Appl. Phys. 82 (1997) 6326.
[14] P.W.M. Blom, M.J.M. De Jong, J.J.M. Vleggaar, Appl. Phys. Lett. 68 (1996) 3308.
[15] P.S. Davids, I.H. Campbell, D.L. Smith, J. Appl. Phys. 82 (1997) 6319.
[16] E.S. Yang, Microelectronic Devices, McGraw-Hill, New York, 1988.
[17] N. Arora, MOSFET Models for VLSI Circuit Simulation: Theory and Practice, Springer, Berlin, 1993.
[18] Y.S. Lee, J.H. Park, J.S. Choi, Opt. Mater. 21 (2002) 433.
[19] J.D. McNeill, D.B. O'Connor, D.M. Adams, P.F. Barbara, S.B. Kammer, J. Phys. Chem. B 105 (2001) 76.
[20] G. Liang, T. Cui, K. Varahramyan, Solid State Electron. 47 (2003) 691.
[21] I.H. Campbell, T.W. Hagler, D.L. Smith, J.P. Ferraris, Phys. Rev. Lett. 76 (1996) 1900.